Mathematical Biosciences 232 (2011) 78–86

Contents lists available at ScienceDirect

Mathematical Biosciences

journal homepage: www.elsevier.com/locate/mbs

Extinction conditions for isolated populations with Allee effect

Vicenç Méndez [a,*], Cristina Sans [a], Isaac Llopis [b], Daniel Campos [a]

[a] Grup de Física Estadística, Departament de Física, Universitat Autònoma de Barcelona, 08193 Bellaterra (Cerdanyola), Spain
[b] Departament de Física i Enginyeria Nuclear, Escola Superior d'Agricultura de Barcelona, Campus del Baix Llobregat. Edifici D4, Universitat Politècnica de Catalunya, 08860 Castelldefels (Barcelona), Spain

ARTICLE INFO

Article history:
Received 12 November 2010
Received in revised form 18 April 2011
Accepted 25 April 2011
Available online 5 May 2011

Keywords:
Critical patch size
Allee effect
Extinction

ABSTRACT

One of the main ecological phenomenons is the Allee effect [1–3], in which a positive benefit from the presence of conspecifics arises. In this work we describe the dynamical behavior of a population with Allee effect in a finite domain that is surrounded by a completely hostile environment. Using spectral methods to rewrite the local density of habitants we are able to determine the critical patch size and the bifurcation diagram, hence characterizing the stability of possible solutions, for different ways to introduce the Allee effect in the reaction–diffusion equations.

1. Introduction

Allee effects occur whenever fitness of an individual in a small or sparse population decreases as the population size or density also declines [1–5]. Even though the terminology involved in the Allee effect classification is still somewhat controversial, a distinction is usually made between 'component' and 'demographic' Allee effects. The first one is defined as a positive relationship between any measurable component of individual fitness and population size or density, whereas the second one designates a positive relationship between total individual fitness and population size or density and is classically measured by the per capita population growth rate [6,7]. In this paper, we will focus on the 'demographic' Allee effect and refer to it simply as the Allee effect for the sake of brevity.

When a population experiences Allee effect, the per capita growth rate of the species is reduced at low density [8], which is also referred to as a positive relationship between population growth rate and density [9] or an inverse density dependence at low population sizes [10]. In other words, the individuals of these species benefit from the presence of conspecifics, cooperate with them; if the lack of conspecifics is stronger than the benefits obtained, then the individuals may be less likely to reproduce or survive at low population sizes and their fitness might be reduced [11]. In consequence, the Allee effect can also be viewed as the disadvantage of too few of conspecifics. So, the Allee effect can also be defined as the failure to mate successfully that occurs when the population density falls below a certain critical threshold.

Allee effects can be either 'strong' or 'weak', although the latter is often ignored [12]. Under the former case, populations experience negative per capita growth rates when density falls beyond the critical threshold, and if a population does not surpass this threshold it will become extinct. Under 'weak' Allee effects, populations experience lower per capita growth rates at low densities but they are always positive, hence there is no critical threshold to be exceeded for the population to survive [8].

There are several reasons why populations may exhibit Allee effects, such as less efficient feeding at low densities, reduced effectiveness of vigilance and antipredator defences, and inbreeding depression [13]. The most cited and obvious case of the Allee effect is the difficulty of finding mates at low population sizes in sexually reproducing species [6], although it represents only a small subset of social causes of inverse density dependence [9]. Directly or indirectly, the ramifications of Allee effects can be seen in almost every area of ecology and conservation, as even species under no obvious Allee effect might be affected by others that do.

Abundant theoretical models account for the Allee effect. Some of them incorporate the Allee effect by multiplying the per capita growth rate by a term that becomes negative when the population density is below a certain threshold and positive otherwise [13], a case known as multiplicative Allee effect. Other models add a predation term which causes the Allee effect, which is known as Holling type II functional response [14].

In this work we want to investigate the role of strong and weak Allee effect on the extinction conditions for a population living in a single patch surrounded by completely hostile conditions. Although the assumption of completely hostile environment represents an idealization, it has been employed traditionally in the literature, not only in general theoretical studies [15–17], but also

* Corresponding author.
E-mail addresses: vicenc.mendez@uab.es, vicenc.mendez@uab.cat (V. Méndez).

0025-5564/$ - see front matter © 2011 Elsevier Inc. All rights reserved.
doi:10.1016/j.mbs.2011.04.005

in models of specific populations such as plankton blooms [18], critical plankton filaments [19], fish populations in marine protected areas [20], annual plants [21] and bacterial colonies under ultraviolet light [22]. If individuals reach the habitat boundaries, they are absorbed, killed or removed instantaneously. Hostile surroundings favor population extinction but, if the net growth rate is high enough to compensate for the losses at the boundaries, persistence is guaranteed.

This problem has been theoretically studied by some authors. Smoller and Wasserman [23], Britton [24] and Cantrell and Cosner [25] studied the bifurcation problem of the steady-state solution of the reaction–diffusion equation. They considered Dirichlet, Neumann and periodic boundary conditions and obtained qualitative bifurcation diagrams by using the technique of the so-called time-map. More recently, Shi and Shivaji [26] used only weak Allee effect but on the other hand also considered higher-dimensional systems. They constructed the bifurcation diagrams qualitatively by analyzing the sub and super-solutions of the steady-state problem. Other studies have included also the effect of density-dependent diffusion [27] or have considered spatial variability [28,29].

To study the role of the Allee effect on the extinction condition for a population living in a one-dimensional patch surrounded by completely hostile conditions we employ the Galerkin spectral method [30]. It allows us to get analytical results for the critical patch size and the coordinates of the bifurcation point that separates the extinction and survival regions. Our method is able to deal consistently with both weak and strong Allee effects and is applied to three different models proposed in the literature. In addition, we can also study analytically the role of the initial central density on the extinction conditions. These results are checked with numerical solutions and cannot be achieved from the previous studies.

2. Galerkin spectral method

A population living in a one-dimensional finite habitat may be modeled by a reaction–diffusion equation with Dirichlet boundary conditions, that is,

$$\frac{\partial \rho}{\partial t} = D\frac{\partial^2 \rho}{\partial x^2} + f(\rho), \quad \text{with} \quad \rho(0,t) = \rho(L,t) = 0, \tag{1}$$

where $0 \leqslant \rho(x,t) \leqslant 1$ is the population density, D is the diffusion coefficient, $f(\rho)$ describes the net population change from birth and death, and hence $f(\rho)/\rho$ stands for the per capita growth rate. The boundary conditions in (1) define a patch of size L surrounded by a completely hostile environment. This model neglects stochastic aspects due to external noise introduced in the system through the fluctuation of a parameter and due to internal noise as consequence of low population densities. The model assumes a continually reproducing population, and an absence of strong interactions with other species.

Spectral methods are a class of techniques used to solve numerically certain partial differential equations (PDEs) [30]. If $\rho(x,t)$ is sufficiently smooth then it admits the series expansion

$$\rho(x,t) = \sum_{n=1}^{\infty} \varphi_n(t)\phi_n(x), \tag{2}$$

where $\phi_n(x)$ is a complete set of functions (preferably orthogonal under some inner product) that satisfy the boundary conditions $\phi_n(0) = \phi_n(L) = 0$. In the Galerkin approach one demands that the residual is orthogonal to the space from which $\rho(x,t)$ comes. This is accomplished by ensuring that the residual is orthogonal to each of the basis functions. Considering $\phi_n(x) = \sin(n\pi x/L)$, from Eq. (1) we define the residual

$$R(x,t) = \frac{\partial \rho}{\partial t} - D\frac{\partial^2 \rho}{\partial x^2} - f(\rho)$$

and require that

$$\int_0^L R(x,t)\sin\left(\frac{m\pi x}{L}\right)dx = \int_0^L \left[\frac{\partial \rho}{\partial t} - D\frac{\partial^2 \rho}{\partial x^2} - f(\rho)\right] \times \sin\left(\frac{m\pi x}{L}\right)dx = 0. \tag{3}$$

Inserting (2) into (3) the evolution equation for the coefficients $\varphi_n(t)$ reads

$$\frac{d\varphi_n}{dt} = -D\left(\frac{n\pi}{L}\right)^2 \varphi_n + \int_0^L f(\rho)\sin\left(\frac{n\pi x}{L}\right)dx. \tag{4}$$

The integral of the right hand side of Eq. (4) can be performed if the expression for the reaction function is known and the functions $\varphi_n(t)$ can be obtained by solving the corresponding nonlinear ordinary differential equations. However, to gain simplicity and analytic results in what follows, let us assume that the first term ($n = 1$) of the expansion (2) is the leading term i.e., it is the main contribution; that is, $\rho(x,t) \simeq \varphi_1(t)\sin(\pi x/L)$. So that, the functions $\varphi_{n>1}(t)$ are supposed to be of higher order than $\varphi_1(t)$. This is the approach we take throughout the reminder of the paper. The validity of this approach is analyzed in detail in the Appendix A at the end of the paper.

Now, the problem is to compute and study the temporal behavior of $\varphi_1(t)$. To do this we approximate $f(\rho)$ by neglecting higher-order nonlinear terms than $f(\varphi_1)$. Let us assume that the reaction term has the form

$$F(\rho) = a_1\rho + a_2\rho^2 + a_3\rho^3. \tag{5}$$

Hence, keeping nonlinear terms up to φ_1^3 in $f(\rho)$, Eq. (4) turns, for $n = 1$, into

$$\frac{d\varphi_1}{dt} = \left[-D\left(\frac{\pi}{L}\right)^2 + a_1\right]\varphi_1 + \frac{8a_2}{3\pi}\varphi_1^2 + \frac{3a_3}{4}\varphi_1^3. \tag{6}$$

The steady-state solutions are

$$\varphi_1 = 0, \tag{7}$$

$$\varphi_1^{\pm} = -\frac{16a_2}{9\pi a_3} \pm \frac{2}{3a_3}\sqrt{\left(\frac{8a_2}{3\pi}\right)^2 - 3a_3\left(a_1 - D\frac{\pi^2}{L^2}\right)}. \tag{8}$$

The above solutions conform the branches of the bifurcation diagram of the central population density as a function of the patch size. To define the regions of stability (survival) or instability (extinction) we insert into (6) $\varphi_1(t) = \varphi_1^* + \epsilon(t)$, where $\epsilon(t)$ is a small perturbation and φ_1^* is any of the solutions given by (7) and (8). We find after linearizing that

$$\varphi_1 = 0 \text{ is stable if } a_1 - D\frac{\pi^2}{L^2} < 0 \tag{9}$$

and

$$\varphi_1^{\pm} \text{ is stable if } \frac{3a_3}{2}\varphi_1^{\pm} + \frac{8a_2}{3\pi} < 0. \tag{10}$$

From (10) and (8) it is seen that φ_1^+ is the stable branch and φ_1^- is unstable branch. As we will see in detail in the next section for any of the examples we study, the unstable branch plays the role of separatrix between the attraction basins of the states $\varphi_1 = 0$ and φ_1^+ such that if the initial central density exceeds φ_1^- then the central density goes to φ_1^+ and population survives. If the central density is below φ_1^- then population extincts. This is what we call relative extinction/survival. As the bifurcation branches correspond to the values of central density φ_1 for different habitat sizes it is not surprising that what is really important of the initial condition is

not how it is distributed along the space but its central value. Recall that under our approach $\rho(x,t) \simeq \varphi_1(t)$ sin $(\pi x/L)$, so that $\varphi_1(t) \simeq \rho(x = L/2, t)$ is the central density and is $\varphi_1(0) \simeq \rho(x = L/2, 0)$ the initial central density. The only conditions that the initial condition must accomplish for numerical calculations are that it must be symmetric respect to $x = L/2$ due to the symmetry of the problem (1) so that the maximum value of the density must be attained at $x = L/2$.

In the next sections we examine the conditions for extinction and survival for different models of Allee effects proposed in the literature distinguishing between strong and weak Allee effects. From (5) this difference can be established as

$$\begin{aligned} &\text{weak Allee effect}: a_1 > 0, \\ &\text{strong Allee effect}: \frac{a_2^2}{4a_3} < a_1 < 0. \end{aligned} \tag{11}$$

3. Multiplicative Allee effect

In this section we apply the above analysis to the case of multiplicative Allee effect. The pioneer model was proposed by Lewis and Kareiva [13]; there the per capita growth rate was multiplied by $(1-\rho)(\rho-\rho_0)$. Note that the Allee effect is present when $0 < \rho_0 < 1$ and if $\rho < \rho_0$ the per capita growth rate becomes negative. So, ρ_0 represents the fraction of carrying capacity below which the ill-effects of a low population density produce a negative growth. The less ρ_0 is, the less prominent is the Allee effect. In this section we make use of a slight variation of this model [31] that can deal with both weak and strong Allee effect:

$$f(\rho) = \rho[r - b(\rho - a)^2], \tag{12}$$

where a, b and r are positive parameters and the carrying capacity is taken to be 1. From the criteria (11) the Allee effect is weak if $r > a^2 b$ and strong if $r < a^2 b$. For population densities ρ below the threshold $\rho^\dagger \equiv a - \sqrt{r/b}$ the population growth becomes negative. In consequence, $\rho^\dagger$ plays the role of ρ_0 in the model by Lewis and Kareiva. To study the stability of the different solutions in the bifurcation diagram we need to consider separately the cases with weak or strong Allee effect.

3.1. Weak Allee effect ($r > a^2 b$)

From (9), (10) and (12) the extinction state (7) is stable if $L < L_c$ and unstable if $L > L_c$, where

$$L_c = \pi\sqrt{\frac{D}{r - a^2 b}}, \tag{13}$$

that is always larger than for a logistic growth ($a = 0$)

Analogously, it can be shown that the state φ_1^+ is stable and φ_1^- is unstable, being

$$\varphi_1^{\pm} = \frac{32a}{9\pi} \pm \frac{2}{3b}\sqrt{\left(\frac{16ab}{3\pi}\right)^2 + 3b\left(r - a^2 b - D\frac{\pi^2}{L^2}\right)}. \tag{14}$$

As both branches join at the bifurcation point, $\varphi_1^+ = \varphi_1^-$, the coordinates of the bifurcation point are, from (14), given by

$$\varphi_1^{(b)} = \frac{32a}{9\pi}, \tag{15}$$

$$L_b = \pi\sqrt{\frac{D}{\frac{1}{3b}\left(\frac{16ab}{3\pi}\right)^2 + r - a^2 b}}. \tag{16}$$

In Fig. 1 we plot the analytical results given by (14) together with numerical calculations. The latter are performed by using a centered finite difference scheme. The agreement between both confirms that the approach of considering the first term only is reasonable. The figure shows a backward bifurcation where $\varphi_1^{(b)}$ is the minimal survival population density. When the patch size is lower than L_b the population becomes extinct, but when $L_b < L < L_c$ both extinction and survival solutions are stable. In this case the final population density depends on the value of the initial central density. Population extincts if $\varphi_1(0) < \varphi_1^-$ and survives otherwise. Therefore the solution φ_1^- plays the role of separatrix between the attraction basin of the extinction and survival states. Moreover, as φ_1^- decreases with L, the greater L the less initial central density is necessary for survival. If the patch size surpasses $L_c$then population will always survive for any initial density profile.

The coordinates of the bifurcation point, obtained analytically in (15) and (16), have been also compared to numerical solutions in Fig. 2. It is seen how L_b increases with a (region $0 < a < 0.55$). This

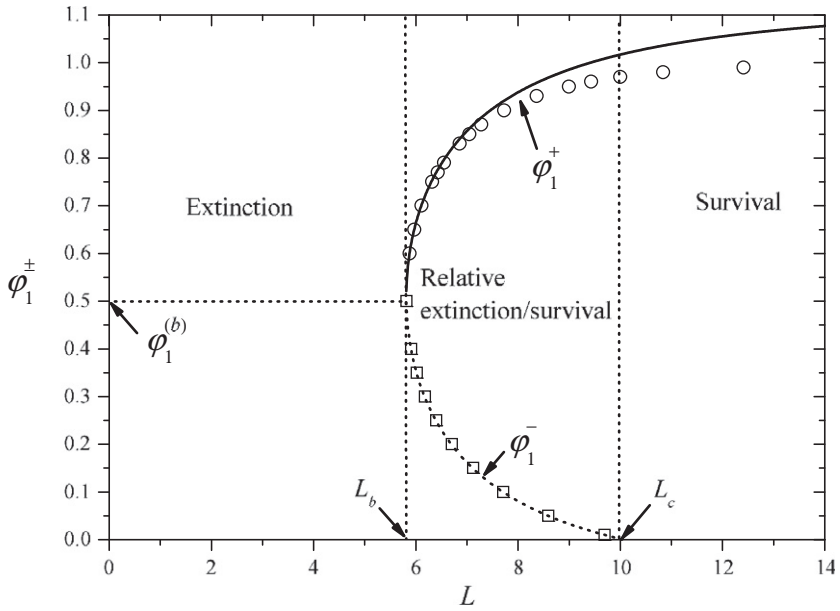

Fig. 1. Backward bifurcation for weak multiplicative Allee effect. If $L < L_b$ population becomes extinct. The solid (stable) curve corresponds to the positive solution given in (14) and the dotted (unstable) curve corresponds to the negative solution. The symbols correspond to the numerical solutions. $D = b = 1$, $a = 0.55$ and $r = 0.4$.

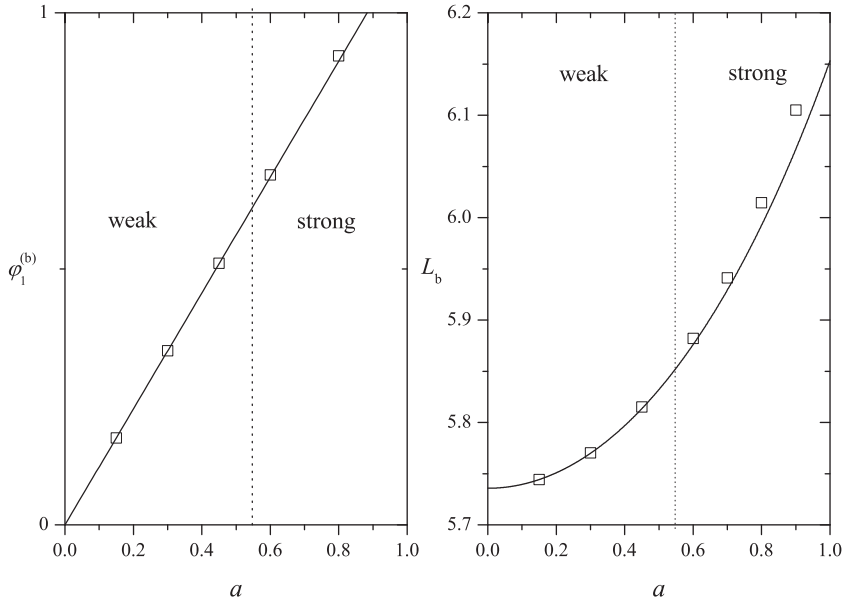

Fig. 2. Dependence of the population density and the patch size at the bifurcation point as function of a. Solid curves correspond to the analytical results given in (15) and (16) and the squares are the numerical results. We have considered $D = b = 1$ and $r = 0.3$. The region $0 < a < 0.55$ corresponds to weak Allee effect while the region $a > 0.55$ corresponds to strong Allee effect.

parameter denotes how strong the Allee effect is, so that the extinction region expands to the right (due to the growth of L_b) when a increases, as expected. The population density at the bifurcation point, $\varphi_1^{(b)}$, increases almost linearly with a.

3.2. Strong Allee effect ($r < a^2 b$)

In this case the condition (9) is always satisfied so that the extinction state is always stable, regardless of the patch size. The region of survival, present for weak Allee effect when $L > L_c$, is thus not present here and φ_1^- decreases as L increases but never reaches the value zero. Then, the bifurcation diagram has only two regions: the extinction region when $L < L_b$ and the relative extinction/survival region for $L > L_b$. In consequence, under a strong Allee effect, a population can survive only if the patch is larger than L_b and if the initial central population density is higher than φ_1^-. If one or both of these conditions are not met, then the population becomes extinct. In Fig. 3 we represent a bifurcation diagram for this case, which illustrates these comments. In Fig. 2 we have also plotted the coordinates of the bifurcation point (region $a > 0.55$).

An interesting comparison can be made between these results for the strong Allee effect and those one would find in a well-mixed media (that is, without diffusion of individuals). In that case one would have that the population will go extinct if the population density falls below the threshold density $\rho^\dagger$. Since the hostile environment introduces even more restrictive conditions for population growth (all the individuals that cross the domain boundaries disappear) one would expect that extinction is still more likely. However, this is not necessarily the case due to the fact that the hostile conditions lead to a spatially structured population. This can be seen by comparing the average density

$$\frac{1}{L}\int_0^L \rho(x,t)dx \simeq \frac{2\varphi_1}{\pi} \tag{17}$$

with the threshold density $\rho^\dagger$. Near the bifurcation point one can replace (15) and (16) into (17). Then one has that in the vicinity of the bifurcation point the average population can be below the density threshold $\rho^\dagger$ provided that

$$D < \left(\frac{9\pi}{64a}\right)^2 \left(a - \sqrt{\frac{r}{b}}\right)^2 \left(\frac{1}{3b}\left(\frac{16ab}{3\pi}\right)^2 + r - a^2 b\right). \tag{18}$$

In that case the stationary population density will be, in average, below the critical value but the population will still survive. The interpretation of Eq. (18) is quite straightforward: a slow dispersal rate will make the population mixing very slow, so near the central part ($x = L/2$) of the domain where the density is high, the population can persist even if near the (hostile) boundaries the population is very small.

4. Shifted logistic growth

In this section we deal with a growth function of the form

$$f(\rho) = r\rho^\beta(1-\rho), \tag{19}$$

that has been applied for populations of whales [32,33] or forest fire models [34]. The parameter $\beta > 1$ measures the difficulty of the mating process. In forest fire models it expresses the number of burning trees necessary to set fire to a green tree. Then, the greater $\beta$the more prominent the Allee effect is. At first sight one could think that this is a case of weak Allee effect because, as can be seen from (19), the population and the per capita growth rate is 0 at $\rho = 0$. However, as we show below the corresponding bifurcation diagram and its properties are qualitatively equal to the case of strong Allee effect. By combining (4) with (19) one gets, for $n = 1$,

$$\frac{d\varphi_1}{dt} = -D\left(\frac{\pi}{L}\right)^2 \varphi_1 + rM\varphi_1^\beta - rN\varphi_1^{\beta+1}, \tag{20}$$

where

$$M = \frac{\Gamma(2+\beta)}{2^\beta \Gamma\left(\frac{3+\beta}{2}\right)^2}, \quad N = \frac{\Gamma(3+\beta)}{2^{1+\beta}\Gamma\left(\frac{4+\beta}{2}\right)^2}$$

and $\Gamma(\,)$ is the Gamma function. As $\beta > 1$ the state of extinction $\varphi_1 = 0$ is always stable. In this case there is no critical patch size and the bifurcation diagram is similar to that of Fig. 3. First, let us compute the coordinates of the bifurcation point. The solution for the state of relative survival/extinction is obtained by setting the

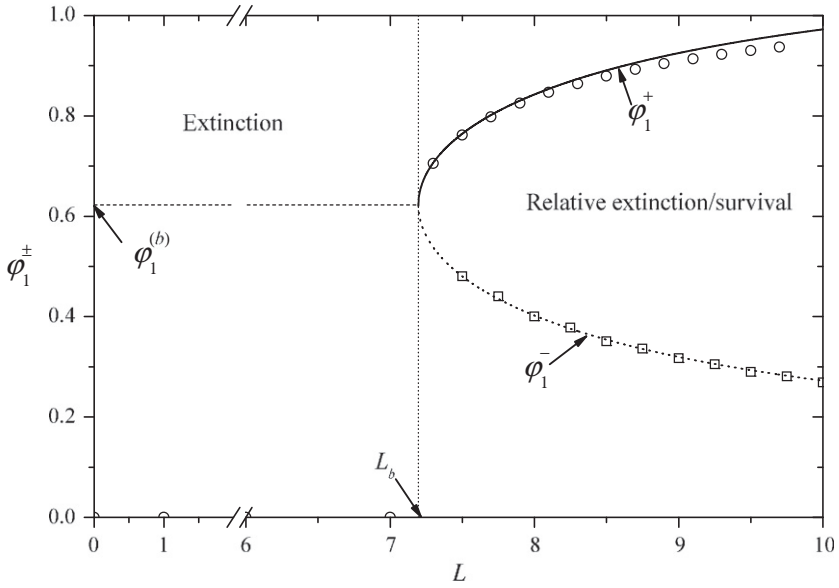

Fig. 3. Backward bifurcation for strong multiplicative Allee effect. The solid (stable) curve corresponds to the positive solution given in (14) and the dotted (unstable) curve corresponds to the negative solution. The symbols correspond to the numerical solutions. $D = b = 1$, $a = 0.55$ and $r = 0.05$.

right hand side of Eq. (20) equal to zero. This equation can be rewritten by solving for L

$$L = \pi\sqrt{\frac{D}{r}}\frac{1}{\varphi_1^{\frac{\beta-1}{2}}\sqrt{M - N\varphi_1}}. \tag{21}$$

The bifurcation point satisfies $\partial L/\partial\varphi_1 = 0$. Solving this equation for φ_1 and inserting the result into (21) one finds

$$\varphi_1^{(b)} = \frac{2(\beta-1)}{\beta(2+\beta)}\left[\frac{\Gamma\left(\frac{4+\beta}{2}\right)}{\Gamma\left(\frac{3+\beta}{2}\right)}\right]^2, \tag{22}$$

$$L_b = \pi\sqrt{\frac{2D}{r}}\left(\frac{\beta-1}{2+\beta}\right)^{\frac{1-\beta}{2}}\beta^{\beta/2}\frac{\Gamma\left(\frac{3+\beta}{2}\right)^{\beta}\Gamma\left(\frac{4+\beta}{2}\right)^{1-\beta}}{\Gamma(2+\beta)^{1/2}}. \tag{23}$$

In the limit $\beta \to 1$, (19) tends to the logistic growth, $\varphi_1^{(b)} \to 0$ and $L_b \to \pi\sqrt{D/r}$ [15]. For $\beta = 2$ it is easy to find an analytic solution for the bifurcation diagram. Setting $\beta = 2$ in (20), equating to zero and solving for φ_1, one finds

$$\varphi_1^{\pm} = \frac{16}{9\pi} \pm \frac{1}{2}\sqrt{\left(\frac{32}{9\pi}\right)^2 - \frac{16D\pi^2}{3rL^2}}. \tag{24}$$

In Fig. 4 we plot the bifurcation diagram for the central population density as a function of the patch size. As can be seen, it is qualitatively equal to that corresponding to strong Allee effect. If $L < L_b$ population becomes extinct. The extinction/survival is conditioned again by the amplitude of the initial central density condition. If $\varphi_1(0) > \varphi_1^-$ the population survives and the central density evolves towards φ_1^+. Contrarily, if $\varphi_1(0) < \varphi_1^-$ the population becomes extinct. In Fig. 5 we plot the coordinates of the bifurcation point given in (22) and (23) as function of the parameter β, that is a measure of how prominent the Allee effect is. Similarly to the previous case with a, the parameters $\varphi_1^{(b)}$ and L_b are increasing functions of β.

5. Logistic growth with a cutoff

The logistic growth with a cutoff at low densities can be written as

$$f(\rho) = r\theta(\rho - a)\rho(1-\rho), \tag{25}$$

where $\theta(\cdot)$ is the Heaviside function, that is, $\theta(\rho - a) = 0$ if $\rho < a$ and $\theta(\rho - a) = 1$ if $\rho > a$. The growth function (25) has been considered to model the effect of stochastic fluctuations that appear when the density of individuals in a population is small [35]. This is also known as internal or demographic fluctuations. From an ecological perspective the parameter a plays the role of a threshold density. When the population density falls below a then population growth breaks down due to mating difficulties that appears at low population densities. This growth function can be used to study the role of internal fluctuations in front propagation [35] and the epidemic waves [36]. Inserting (25) into (4), the integral can be carried out for $n = 1$

$$\begin{aligned}\int_0^L f(\rho)\sin\left(\frac{\pi x}{L}\right)dx &\simeq \frac{2L}{\pi\varphi_1^2}\int_a^{\varphi_1}\frac{\rho^2(1-\rho)}{\sqrt{1-\frac{\rho^2}{\varphi_1^2}}}d\rho \\ &= \frac{2L}{\pi}\varphi_1\int_{a/\varphi_1}^1\frac{s^2(1-\varphi_1 s)}{\sqrt{1-s^2}}ds = \frac{2L}{\pi}\varphi_1\left[\frac{\pi}{4} - \frac{1}{2}\arcsin\left(\frac{a}{\varphi_1}\right)\right. \\ &\quad \left. + \left(\frac{a}{2\varphi_1} - \frac{2\varphi_1}{3} - \frac{a^2}{3\varphi_1}\right)\sqrt{1-\frac{a^2}{\varphi_1^2}}\right].\end{aligned} \tag{26}$$

In the first step of the calculation above we have performed the change of variable $\sin(\pi x/L) \simeq \rho/\varphi_1$ and in the second step we define $s = \rho/\varphi_1$. By introducing (26) into (4) with $n = 1$ we get the evolution equation

$$\begin{aligned}\frac{d\varphi_1}{dt} &= -D\left(\frac{\pi}{L}\right)^2\varphi_1 \\ &\quad + \frac{4r}{\pi}\left[\frac{\pi\varphi_1}{4} - \frac{\varphi_1}{2}\arcsin\left(\frac{a}{\varphi_1}\right) + \left(\frac{a}{2} - \frac{2\varphi_1^2}{3} - \frac{a^2}{3}\right)\sqrt{1-\frac{a^2}{\varphi_1^2}}\right]\end{aligned} \tag{27}$$

for φ_1. The nontrivial solution, corresponding to the relative survival, is defined by equating to zero the right hand side of (27). As the resulting equation cannot be solved for φ_1, we solve it for L:

$$L = \pi\sqrt{\frac{D}{r}}\frac{1}{\sqrt{G(\varphi_1)}}, \tag{28}$$

where

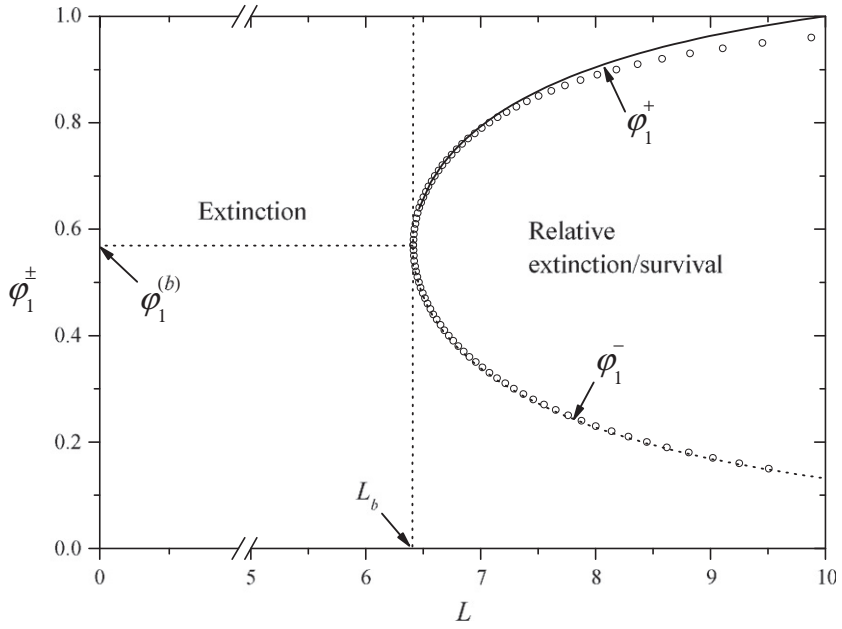

Fig. 4. Bifurcation diagram for shifted logistic growth. $D = r = 1$ and $\beta = 2$. The solid (stable) and dotted (unstable) curves correspond to the solutions given in (24) and symbols correspond to numerical solutions.

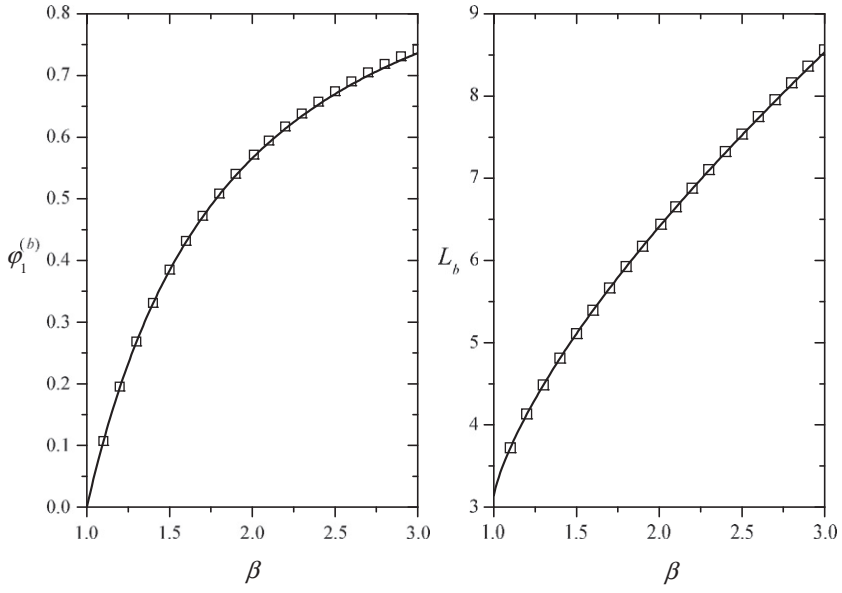

Fig. 5. Dependence of the population density and the patch size at the bifurcation point as function of $\beta$for the shifted logistic growth. Solid curves correspond to the analytical results given in (22) and (23) and squares are the numerical results. We have considered $D = r = 1$.

$$G(\varphi_1) \equiv 1 - \frac{2}{\pi}\arcsin\left(\frac{a}{\varphi_1}\right) + \frac{4}{\pi}\left(\frac{a}{2\varphi_1} - \frac{2\varphi_1}{3} - \frac{a^2}{3\varphi_1}\right)\sqrt{1 - \frac{a^2}{\varphi_1^2}}. \tag{29}$$

The bifurcation point can be obtained, as in the previous case, by solving $\partial L/\partial\varphi_1 = 0$ to get

$$\varphi_1^{(b)} = \frac{\sqrt{a}}{2}\sqrt{a + \sqrt{3a}\sqrt{8 - 5a}}, \qquad L_b = \pi\sqrt{\frac{D}{r}}\frac{1}{\sqrt{G(\varphi_1^{(b)})}}. \tag{30}$$

In Fig. 6 we plot the bifurcation diagram for the central population density as function of the patch size. As can be seen, this diagram is qualitatively equal to that for shifted logistic and suggests that in both cases the population is under a strong Allee effect.

Let us check now the stability of the branches of the bifurcation diagram. As for $0 \leqslant \rho < a$ the reaction term vanishes, the equation for any small perturbation $\epsilon(t)$ of the extinction state $\varphi_1 = 0$ follows the ordinary differential equation $d\epsilon/dt = -D\pi^2\epsilon/L$ and $\epsilon(t)$ tends exponentially to zero proving that the state $\varphi_1 = 0$ is globally stable. From Eq. (28) and solving for φ_1 one obtains the two branches, the upper branch φ_1^+ and the lower branch. To analyze the stability let us introduce $\varphi_1(t) = \varphi_1^{\pm} + \epsilon(t)$, with $\epsilon(t)$ a small perturbation, into (27). Expanding and collecting terms the perturbation follows $\epsilon(t) \sim e^{\Lambda t}$ where

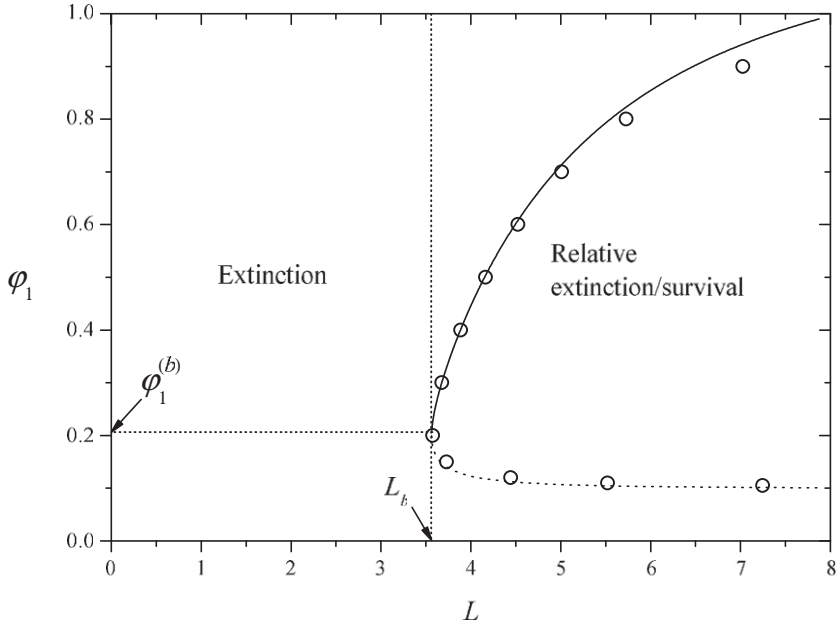

Fig. 6. Bifurcation diagram for logistic growth with cutoff. We have considered $D = r = 1$ and $a = 0.1$. The solid (stable) and dotted (unstable) curves correspond to the solutions given in (28) and symbols corresponds to numerical solutions.

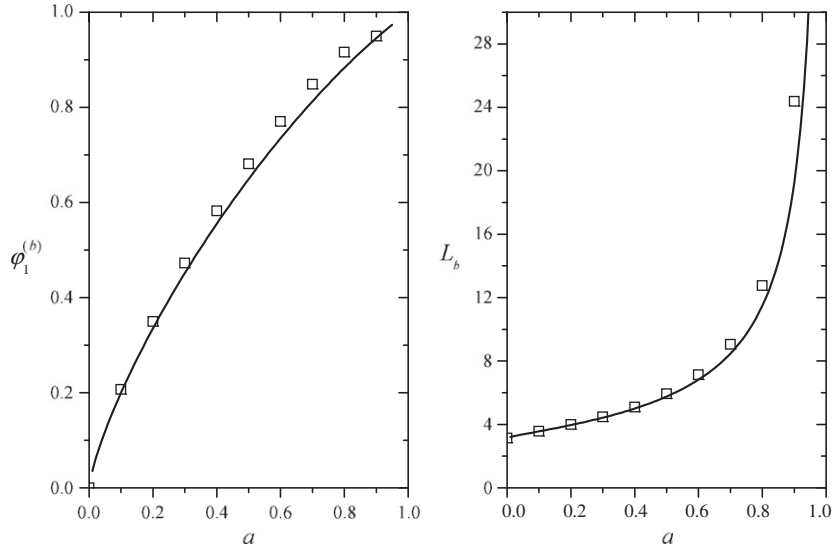

Fig. 7. Dependence of the population density and the patch size at the bifurcation point with a for the logistic growth with cutoff. Solid curves correspond to the analytical results given in (30) and the squares are the numerical results. We have considered $D = r = 1$.

$$\Delta = -D\frac{\pi^2}{L^2} + rG(\varphi_1^{\pm}) + r\varphi_1^{\pm}G'(\varphi_1^{\pm}). \tag{31}$$

To find the sign of Δ let us analyze a point on the branches close to the bifurcation point (30) by setting $L = L_b + \delta_1$. So, we consider a point belonging to the upper branch near the bifurcation point by introducing $\varphi_1^{+} = \varphi_1^{(b)} + \delta_2$ with $\delta_2 > 0$. Analogously, the point belongs to the lower branch if we introduce $\varphi_1^{+} = \varphi_1^{(b)} + \delta_2$ with $\delta_2 < 0$. Then, inserting the above definitions in (28) one has $-2D\pi^2\delta_1 = rG''(\varphi_1^{(b)})\delta_2^2/2$ and inserting them in (31)

$$\Delta \simeq r\varphi_1^{(b)}G''(\varphi_1^{(b)})\delta_2 + O(\delta_2^2),$$

where we have made use of $\partial L/\partial\varphi_1 = 0$ (i.e., $G'\left(\varphi_1^{(b)}\right) = 0$). As $G''\left(\varphi_1^{(b)}\right) < 0$ (this can be easily checked from (29) and (30)), the upper branch ($\delta_2 > 0$) has $\Delta < 0$ and is globally stable while the lower branch is unstable.

In Fig. 7 we plot the central population density and the patch size at the bifurcation point as function of the threshold density a. As in previous cases (shifted logistic and strong Allee effect) both the central density and the patch size at the bifurcation point increase as the Allee effect becomes stronger. However, Figs. 2 and 7 differ from Fig. 5 because the concavity of the graph L_b versus a or β. This is due to the way in which L_b increases with the threshold parameter. In Fig. 2 L_b increases with a as $L_b \sim (a_0 - a)^{-1/2}$ but in Figs. 5 and 7 the dependence is more complex.

6. Conclusions

The critical patch size of a population is the minimal size of the habitat necessary for population survival. In this paper we have considered that the population is under Allee effects (strong and

weak) and have found the conditions under which the population either becomes extinct or survives.

In previous studies the bifurcation diagrams had been obtained qualitatively. Here, we have made use of the Galerkin spectral method to get analytical approximate expressions for the critical patch size, the coordinates of the bifurcation point and the branches of the bifurcation diagram. This method is also useful in studying the stability of the branches and to establish the regions of relative extinction/survival in terms of the value of the initial central density. The analytical results are checked with numerical solutions and good accuracy is found. We have computed the bifurcation diagram for the case of multiplicative (weak and strong) Allee effect, shifted logistic growth and logistic growth with a cutoff. We have found that when the critical patch size does not exist ($f'(0) \leqslant 0$) the population behaves as under a strong Allee effect: it becomes extinct if the patch size is lower than the value at the bifurcation point L_b and survives otherwise, but only if the amplitude of the initial central density condition exceeds some threshold value that depends on the patch size (relative survival). This happens when the population growth is modeled with a shifted logistic or a logistic with a cutoff. Conversely, when the model exhibits a critical patch size ($f'(0) > 0$), the region of relative survival only takes place if $L_b < L < L_c$, because for $L > L_c$ the population survives regardless of the initial central density condition.

Although the method provides analytical results, and this is a clear advantage with respect to previous studies, it is not exact. Our approach consists in truncating the Galerkin expansion at first order neglecting higher order terms. As we have shown in the Appendix A, this is strictly valid for small values of the population density. As can be appreciated in Figs. 1, 3, 4 and 6 the deviation between our analytical prediction and the numerical results becomes evident as the central density approaches 1. Since the population is spatially structured, we have also found (Section 3.2) that for average densities below the threshold ρ^+ (for which the population growth rate becomes negative) the population is still able to survive.

The hostile environment condition we have assumed in this work (Dirichlet boundary conditions) has been employed in plankton blooms [15], critical plankton filaments [19], fish populations in marine protected areas [20], annual plants [21] and bacterial colonies under ultraviolet light [22]. In conclusion, our predictions could be directly applied to the above systems when they experience strong or weak Allee effects. It remains to be seen, however, how the effect of other boundary conditions (e.g. partially hostile, zero flux or other) will affect (positively or negatively) the spatial dynamics of species with Allee effect. This would be useful, for example, to study the effect on stream populations or rivers [37]. It would be also interesting to study in future works how other patterns of movements as congregation (aggregation as a result of behavioral responses of organisms to conspecifics) compete with Allee effects to avoid the extinction.

Acknowledgments

The work has been funded by Direcció General de Recerca- Generalitat de Catalunya under Grant 2009SGR-164 (V.M. and D.C.) and by MICINN Grant No. FIS2009-13370-C02-01 (V.M.).

Appendix A

In this appendix we check the validity of neglecting $\varphi_{n>1}$ in comparison with φ_1. As we will see, this approximation is better as $\varphi_1 \to 0$. Introducing $F(\rho) = a_1\rho + a_2\rho^2 + a_3\rho^3$ in (4) and keeping nonlinear terms up to order φ_1^3 one gets

$$\frac{d\varphi_n}{dt} = \left[-D\left(\frac{n\pi}{L}\right)^2 + a_1\right]\varphi_n + M_n a_2 \varphi_1^2 + N_n a_3 \varphi_1^3 \tag{32}$$

with

$$M_n = \frac{2}{L}\int_0^L \sin^2\left(\frac{\pi x}{L}\right)\sin\left(\frac{n\pi x}{L}\right) = \frac{4}{n\pi}\frac{(-1)^n - 1}{n^2 - 4},$$

$$N_n = \frac{2}{L}\int_0^L \sin^3\left(\frac{\pi x}{L}\right)\sin\left(\frac{n\pi x}{L}\right) = \frac{12}{\pi}\frac{\sin(n\pi)}{(n^2-9)(n^2-1)}.$$

Let us assume φ_1 small. Then, setting $n = 1$ into (32) one gets $\varphi_1(t) \sim \exp(a_1 - D\pi^2/L^2)t$ and integrating (32) one finds ($n > 1$)

$$\begin{aligned}
\varphi_n(t) &= \varphi_n(0)e^{(a_1 - Dn^2\pi^2/L^2)t} + e^{(a_1 - Dn^2\pi^2/L^2)t} \\
&\quad \times \int_0^t dt' \left[M_n a_2 \varphi_1^2(t') + N_n a_3 \varphi_1^3(t')\right] e^{-(a_1 - Dn^2\pi^2/L^2)t'} \\
&\simeq \varphi_n(0)e^{(a_1 - Dn^2\pi^2/L^2)t} + \frac{M_2 a_2}{a_1 + D\frac{\pi^2}{L^2}(n^2-2)} e^{(2a_1 - 2D\pi^2/L^2)t} \\
&\quad + O(\varphi_1^3) \\
&= A_n \varphi_1^s + B_n \varphi_1^2 + O(\varphi_1^3)
\end{aligned}$$

where

$$s = \frac{D(n\pi/L)^2 - a_1}{D(\pi/L)^2 - a_1} > 1$$

for $n > 1$, and A_n and B_n are suitable constants. Finally,

$$\lim_{\varphi_1 \to 0} \frac{\varphi_n}{\varphi_1} = A_n \varphi_1^{s-1} + B_n \varphi_1 + O(\varphi_1^2) = 0,$$

which shows that if φ_1 is small then $\varphi_{n>1}$ and can be neglected.

References

[1] W.C. Allee, Animal Aggregations, A Study in General Sociology, Univ. of Chicago Press, Chicago, 1931.
[2] W.C. Allee, The Social Life of Animals, William Heinemann, London, 1938.
[3] W.C. Allee, A.E. Emerson, O. Park, T. Park, K.P. Schmidt, Principles of Animal Ecology, W.B. Saunders, Philadelphia, 1949.
[4] P.A. Stephens, W.J. Sutherland, R.P. Freckleton, What is the Allee effect?, Oikos 87 (1999) 185
[5] L. Berec, E. Angulo, F. Courchamp, Multiple Allee effects and population management, TREE 22 (2007) 185.
[6] D.S. Boukal, L. Berec, Single-species models of the Allee effect extinction boundaries, sex ratios and mate encounters, J. Theor. Biol. 218 (2002) 375.
[7] M.S. Fowler, G.D. Ruxton, Population dynamic consequences on Allee effects, J. Theor. Biol. 215 (2002) 39.
[8] C.M. Taylor, A. Hastings, Allee effects in biological invasions, Ecol. Lett. 8 (2005) 895.
[9] F. Courchamp, T. Clutton-Brock, B. Grenfell, Inverse density dependence and the Allee effect, TREE 14 (1999) 405.
[10] P.A. Stephens, W.J. Sutherland, Consequences of the Allee effect for behaviours, ecology and conservation, TREE 14 (1999) 401.
[11] F. Courchamp, L. Berec, J. Gascoigne, Allee Effects in Ecology and Conservation, Oxford University, Oxford, 2008.
[12] M. Wang, M. Kot, Speeds of invasion in a model with strong or weak Allee effects, Math. Biol. 171 (2001) 83.
[13] M.A. Lewis, P. Kareiva, Allee dynamics and the spread of invading organisms, Theor. Popul. Biol. 43 (1993) 141.
[14] B. Dennis, Allee effects: population growth, critical density, and the chance of extinction, Nat. Res. Mod. 3 (1989) 481.
[15] J.G. Skellam, Random dispersal in theoretical populations, Biometrika 38 (1951) 196.
[16] E. Bradford, J.P. Philip, Stability of steady distributions of asocial populations dispersing in one dimension, J. Theor. Biol. 29 (1970) 13.
[17] V. Méndez, D. Campos, Population extinction and survival in a hostile environment, Phys. Rev. E 77 (2008) 022901.
[18] H. Kierstead, L.B. Slobodkin, The size of water masses containing plankton blooms, J. Mar. Res. 12 (1953) 141.
[19] A.P. Martin, On filament width in oceanic plankton distributions, J. Plankton Res. 22 (2000) 597.
[20] U. Malvadkar, A. Hastings, Persistence of mobile species in marine protected areas, Fish. Res. 91 (2008) 69.
[21] J. Latore, P. Gould, A.M. Mortimer, Spatial dynamics and critical patch size of annual plant populations, J. Theor. Biol. 190 (1998) 277.

[22] N.M. Shnerb, Extinction of a bacterial colony under forced convection in pie geometry, Phys. Rev. E 63 (2000) 011906.
[23] J. Smoller, A. Wasserman, Global bifurcation of steady-state solutions, J. Differ. Eqn. 39 (1981) 269.
[24] N.F. Britton, Reaction–Diffusion Equations and Their Applications to Biology, Academic, London, 1986.
[25] R.S. Cantrell, C. Cosner, Spatial Ecology Via Reaction–Diffusion Equations, Wiley Series in Mathematical & Computational Biology, 2003.
[26] J. Shi, R. Shivaji, Persistence in reaction–diffusion models with weak allee effect, J. Math. Biol. 52 (2006) 807.
[27] Y.H. Lee, L. Sherbakov, J. Taber, J. Shi, Bifurcation diagrams of population models with nonlinear diffusion, J. Comput. Appl. Math. 194 (2006) 357.
[28] P.L. Chesson, Models for spatially distributed populations: the effect of within-patch variability, Theor. Popul. Biol. 19 (1981) 288.
[29] P.L. Chesson, Scale transition theory with special reference to species coexistence in a variable environment, J. Biol. Dyn. 3 (2009) 149.
[30] J.S. Hesthaven, S. Gottlieb, D. Gottlieb, Spectral Methods For Time-Dependent Problems, Cambridge University, Cambridge, 2007.
[31] L. Edelstein-Keshet, Mathematical Models in Biology, SIAM, Philadelphia, 2005.
[32] J.M. Conrad, C.W. Clark, Natural Resource Economics: Notes and Problems, Cambridge University, 1987.
[33] C.W. Clark, Mathematical Bioeconomic: The optimal Management of Renewable Resources, John Wiley and Sons, 1990.
[34] V. Méndez, J.E. Llebot, Hyperbolic reaction–diffusion equations for a forest fire model, Phys. Rev. E 56 (1997) 6557.
[35] E. Brunet, B. Derrida, Shift in the velocity of a front due to a cutoff, Phys. Rev. E 56 (1997) 2597.
[36] J. Lin, V. Andreasen, R. Casagrandi, S.A. Levin, Traveling waves in a model of influenza A drift, J. Theor. Biol. 222 (2003) 437.
[37] F. Lutscher, E. McCauley, M.A. Lewis, Spatial patterns and coexistence mechanisms in systems with unidirectional flow, Theor. Popul. Biol. 71 (2007) 267.